

In vivo fluorescence microscopy of neuronal activity in three dimensions by use of voltage-sensitive dyes

Jonathan A. N. Fisher

Department of Physics and Astronomy, University of Pennsylvania, Philadelphia, Pennsylvania 19104-6396

Eugene F. Civillico and Diego Contreras

Department of Neuroscience, University of Pennsylvania School of Medicine, Philadelphia, Pennsylvania 19104

Arjun G. Yodh

Department of Physics and Astronomy, University of Pennsylvania, Philadelphia, Pennsylvania 19104-6396

Received June 13, 2003

We report *in vivo* imaging of neuronal electrical activity from superficial layers of the mouse barrel cortex. The measurements have $\sim 16\text{-}\mu\text{m}$ spatial and 3-ms temporal resolution and reach depths of $150\ \mu\text{m}$ below the cortical surface. The depth-dependent differential-fluorescence optical sections of activity are consistent with known cortical architecture and represent an important step toward *in vivo* measurement of functioning complex neural networks. Our observations employ a custom gradient-index lens probe and voltage-sensitive dye fluorescence; the use of epi-illumination rather than dark-field illumination provides the dramatic signal-to-noise improvement necessary for fast three-dimensional imaging. © 2004 Optical Society of America

OCIS codes: 170.1420, 170.2150, 170.2520, 170.3880, 170.6900.

Neurons integrate and transmit information by means of changes in the electrical potential across their membranes. The predominant methods for measuring such activity in neuroscience require electrodes inserted into the tissue. Such methods, however, provide limited spatial information and are invasive. Optical methods capitalizing on changes in the transmembrane electric field visualized through intrinsic signals^{1,2} and voltage-sensitive dyes^{3–5} (VSDs) offer the possibility for simultaneously imaging the activity of many neurons.⁴ This is a key experimental step for investigating more complex neural functions such as learning, memory, and the fast dynamics of the cortical networks on which such functions depend.⁵

Unfortunately, brain tissue scattering⁶ and the small signal-to-noise ratio ($<1\%$) of optical measurements limit the depth penetration and require long integration times.^{7–9} Experiments with intrinsic signals^{1,2} employ dark-field illumination^{1,8} to detect variations in cellular morphology, either measured as a change in cell volume⁷ or as a change in extracellular space.⁸ These studies typically integrate the responses of the first few hundred micrometers of tissue below the surface. In contrast, most fluorescence microscopy has been limited to nonspecific two-dimensional surface measurements ($25\text{-}\mu\text{m}$, 2.5-ms resolution) of neuronal activity *in vivo*⁹ and *in vitro*.^{5,10} More recently, multiphoton microscopy schemes have demonstrated improved depth of penetration,^{11,12} but signal-to-noise considerations have limited their application to slower processes in the brain, with a limited field of view.¹³ Finally, diffuse optical methods¹⁴ show promise for detecting changes in deep structures of brain tissue but have poorer spatial resolution than the microscopies.

Here we report three-dimensional *in vivo* epifluorescence functional microscopy of neuronal activity in layers one through three of the mouse barrel cortex,

a region of the primary somatosensory cortex where the whiskers are represented. The measurements had $\sim 16\text{-}\mu\text{m}$ spatial resolution in the specimen plane, 3-ms temporal resolution, and probed to depths of $\sim 150\ \mu\text{m}$ below the cortex surface with a transverse field of view of approximately $1.3\ \text{mm} \times 2\ \text{mm}$. The depth-dependent differential images were consistent with known cortical architecture. To our knowledge these are the first *in vivo* optically sectioned neuronal activity measurements based on VSD fluorescence. The microscopy employed a custom gradient-index (GRIN) lens probe. A critical improvement over previous work¹⁵ was the use of epi-illumination rather than dark-field illumination.

In Fig. 1 we show our microscope configuration; the setup allowed us to alternate between dark-field (Fig. 1b) and epi-illumination (Fig. 1a) and to compare the two illumination schemes. Following the pioneering work of Rector *et al.*,¹⁵ we used a GRIN lens objective as the heart of our system. GRIN lenses have been utilized for *in vivo* endoscopy in numerous studies,^{15,16} in part because of their ability to reduce vibration artifacts by direct contact with the brain surface. GRIN lenses are also well suited for fluorescence microscopy of neuronal networks because they offer the combination of small magnification ($\times 3$) and high numerical aperture. The total lens length was 160 mm. The numerical aperture of 0.42 yielded a depth of field (in fluorescence mode) of $6.8\ \mu\text{m}$. A Verdi laser (Coherent, Inc.) operating at 532 nm was used for excitation, illuminating the entire field of view in epi-illumination and dark-field configurations. A secondary objective relayed the inverted image through the emission filters (RG695 glass absorption filters) and onto the CCD. The dark-field illumination utilized excitation light coupled through parallel fibers ($250\text{-}\mu\text{m}$ -core multimode) surrounding the perimeter of the lens (inset, Fig. 1b).

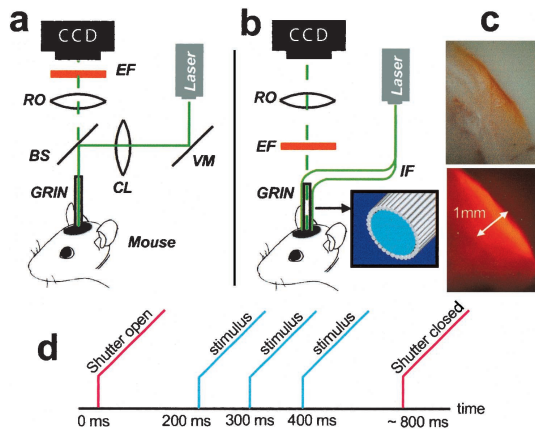


Fig. 1. Optics setup for, a, epifluorescence and, b, dark-field illumination schemes. Inset in b, detail of perimeter fiber illumination. c, Cross-section of RH795-stained brain slice (top, bright field; bottom, fluorescence) revealing uniform staining. d, Time course of events for single trial. BS, beam splitter; CL, collimating objective; RO, relay objective; EF, emission filter; VM, vibrating mirror; IF, illuminating fibers.

For epi-illumination, fiber-coupled excitation light was collimated with a two-element condenser lens and reflected into the GRIN lens by a dichroic mirror (long pass >545 nm). For epi-illumination, laser light was reflected from a vibrating mirror to reduce speckle.

Images were recorded with a MiCam 64×96 pixel 14-bit CCD camera (Brain Vision, Inc., Tsukuba, Japan) with a pixel area of $12 \mu\text{m}^2$ and frame rates above 1 kHz. The $16\text{-}\mu\text{m}$ spatial resolution was limited by the CCD pixel size. The maximum integration time per frame was 3 ms (333-Hz frame rate). Frames of optical data were acquired as differences in fluorescence from a 14-bit reference image, F , (the first frame in the movie) on-line. This yielded a movie consisting of frames that show ΔF . To correct for irregularities in staining, these frames were divided by the reference image off-line to produce fractional fluorescence data ($\Delta F/F$). RH795 (Molecular Probes, 530/712 nm in methanol) exhibited a spectral emission shift in response to depolarization, and ΔF was typically negative. Because our CCD was gray scale, this spectral shift was measured as variation in intensity (ΔF).

The mice were anesthetized with a combination of ketamine and xylazine (100 and 20 mg/kg, respectively, intraperitoneally), a 5-mm-diameter craniotomy was performed, the dura was removed, and the surface of the brain was exposed. Tungsten microelectrodes were placed in the cortex and the thalamus for recording and electrical stimulation. The exposed surface of the barrel cortex was stained with RH795 for ~ 45 min. The cortex was then washed with saline solution to remove unbound dye. Staining was fairly homogeneous as determined from sliced cross sections of the brain examined after the experiments (Fig. 1c).

The experimental timing sequence is shown in Fig. 1d. Trials were separated by a rest period of 6 s. To increase the signal-to-noise ratio, optical recordings of multiple identical trials (10–30 depending on signal

size) were averaged frame by frame. Only one focal plane was imaged per set of single-layer averages, but the order in which the layers were imaged was random.

In Fig. 2 we display images of $\Delta F/F$ from recordings at 0, 75, and $150 \mu\text{m}$ below the cortical surface. All images were processed spatially with a 3×3 Gaussian smoothing filter. The time traces in Fig. 2 were smoothed temporally with a three-frame sliding window filter. Image processing was performed only to clarify large scale qualitative changes in neuronal activity. The time traces represent changes in fluorescence derived from all pixels thresholded below -0.3% . The frames and traces display neuronal activity in response to single electrical stimuli of the cortex (Figs. 2a and 2c) and the thalamus (Figs. 2b and 2d). Each led to qualitatively different three-dimensional spatiotemporal activation of the cortex. In Figs. 2a and 2b a series of nonconsecutive frames shows the response to a single stimulus. Pixel-averaged $\Delta F/F$ time traces in Figs. 2c and 2d are derived from all frames.

The cortex is laminar, and the cellular architecture varies with depth. Since fluorescence is emitted from essentially all stained tissue, software tools were used to reduce the contributions from out-of-plane

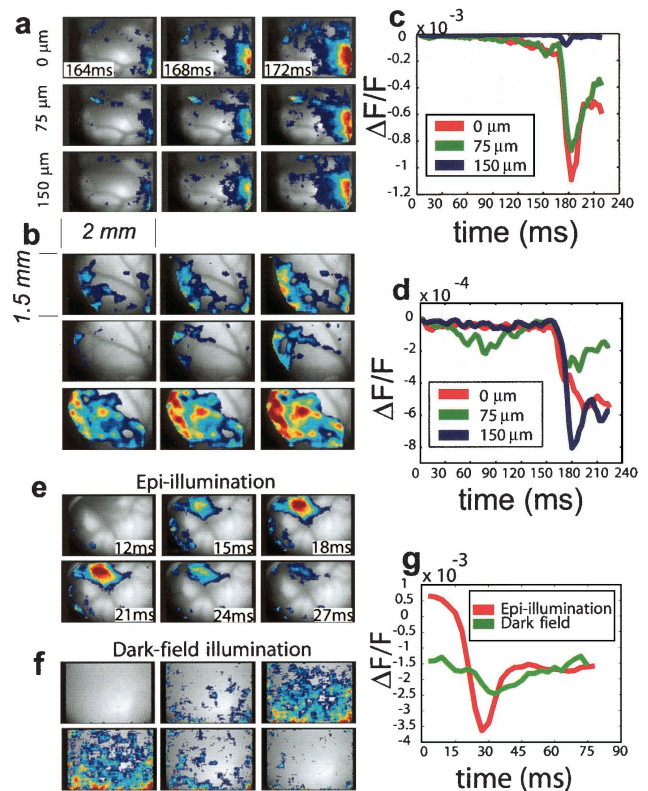


Fig. 2. Neural activity in response to, a, cortical and, b, thalamic stimulation. Stimulation at 150 ms for a, b and 0 ms for e, f. Time stamps for b as in a, f as in e. Frames from left to right: $\Delta F/F$ one frame after stimulation, halfway up the rising edge of the response, and maximum $\Delta F/F$. Traces of averaged, thresholded activity (c, cortical, d, thalamic) show trends as a function of depth. e, illumination Epi-illumination and, f, dark-field-illumination responses to thalamic activity. g, Signal-to-noise comparison.

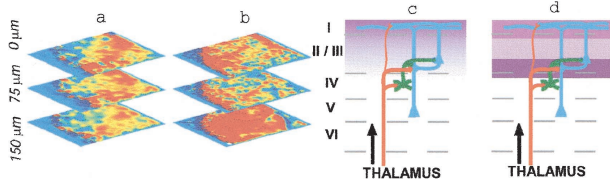


Fig. 3. Peak response $\Delta F/F$ images at three focal planes 0, 75, and 150 μm below the cortex surface during the spread of electrical stimulation (a, cortical; b, thalamic). c, Known thalamocortical and, d, intracortical projections. Shading shows approximate range of GRIN lens measurements with respect to cortical layers and indicates the strength relative to the amplitude of the responses to, c, cortical and, d, thalamic stimulation.

fluorescence. To this end, we employed a computational deconvolution procedure developed by Yae *et al.*¹⁷ This algorithm required an experimentally measured point-spread function at varying depths of defocus as an input parameter.¹⁸ Experimental point-spread functions were obtained by the imaging of fluorescent beads (3- μm diameter) *in situ* at varying degrees of defocus. Our deconvolution techniques resulted in a reduced fractional fluorescence level as well as an increase in the signal-to-noise ratio in plots of pixel value versus time.

The discriminating power of the optical device is illustrated in Fig. 3. We exhibit three of the image planes during responses to single electrical stimuli applied to the cortex in the vicinity of the recording area and to the ventrobasal nucleus of the thalamus. Images of $\Delta F/F$ following cortical stimulation (Fig. 3a) showed a band of activation along the field of view stretching away from the stimulation electrode. The highest response amplitude was at the surface, and it decreased smoothly with depth. In contrast, the response to thalamic stimulation (Fig. 3b) showed a much more widespread area of activation with the highest values at 150- μm depth, limited immediately above (at 75 μm) by the lowest response values, and finally by intermediate fluorescence values at the surface.

Such distribution of activity is compatible with the known anatomy and physiology of the superficial layers of the cortex,¹⁹ in particular with the geometry of cortical cells and the distribution of inputs. Clearly the novel optical probe is capable of spatiotemporally distinguishing layer-dependent physiological responses.

Finally, we compared epi-illumination and dark-field illumination schemes. *A priori*, the detrimental effects of speckle and reflected background light were not known. Figure 2e shows epi-illumination and dark-field-illumination $\Delta F/F$ recordings of the cortical surface in response to a single stimulus of the thalamus averaged over ten trials. The plots in Fig. 2f exhibit corresponding pixel-averaged $\Delta F/F$ traces for each case; the selected pixels are at the center of the activity. The signal-to-noise ratio of the epi-illumination trace was nearly an order of

magnitude larger than the corresponding dark-field recording. In the dark-field illumination scheme, only light backscattered off tissue at and below the image plane returned through the GRIN lens and was detected. To reach an appreciable signal, significantly higher levels of illumination are required in dark-field-illumination ($\sim 500 \text{ mW/cm}^2$) compared with epi-illumination ($\sim 100 \text{ mW/cm}^2$). Our results suggest that in VSD-based fluorescence measurements too much illumination light is lost in dark-field.

To conclude, we have demonstrated epi-illumination, GRIN-lens-based, three-dimensional *in vivo* fluorescence microscopy of neural activity by use of VSDs. To our knowledge these are the first *in vivo* optically sectioned neural activity measurements.

We thank D. M. Rector and J. S. George for extensive discussions about imaging; T. Elam and H. W. Borders for technical assistance; and B. M. Salzberg, L. Finkel, S. M. Potter, and E. Gratton for useful general discussion. Animal procedures were performed in accordance with National Institutes of Health guidelines. Research was supported by the David and Lucille Packard Foundation grant 2000-01737. J. Fisher's e-mail address is aafisher@sas.upenn.edu.

References

1. R. A. Stepnoski, A. LaPorta, F. Raccuia-Behling, G. E. Blonder, R. E. Slusher, and D. Kleinfeld, *Proc. Natl. Acad. Sci. USA* **88**, 9382 (1991).
2. A. Grinvald, E. Lieke, R. D. Frostig, C. D. Gilbert, and T. N. Weisel, *Nature* **324**, 361 (1986).
3. L. B. Cohen and B. M. Salzberg, *Rev. Physiol. Biochem. Pharmacol.* **83**, 35 (1978).
4. R. Yuste, F. Lanni, and A. Konnerth, *Imaging Neurons* (Cold Spring Harbor Laboratory, New York, 2000).
5. D. Contreras and R. Llinas, *J. Neurosci.* **21**, 9403 (2001).
6. F. Bevilacqua, D. Pigué, J. D. Gross, B. J. Tromberg, and C. Depeursinge, *Appl. Opt.* **38**, 4939 (1999).
7. R. Andrew and B. Mac Vicar, *Neurosci.* **62**, 371 (1994).
8. J. Holthoff and O. Witte, *J. Neurosci.* **16**, 2740 (1996).
9. C. C. H. Peterson, A. Grinvald, and B. Sakmann, *J. Neurosci.* **23**, 1298 (2003).
10. R. Yuste, D. W. Tank, and D. Kleinfeld, *Cereb. Cortex* **7**, 546 (1997).
11. K. H. Kim, C. Buehler, and P. T. C. So, *Appl. Opt.* **38**, 6004 (1999).
12. K. Svoboda, F. Helmchen, W. Denk, and D. Tank, *Nat. Neurosci.* **2**, 65 (1999).
13. M. Oheim, E. Beaurepaire, E. Chaigneau, J. Mertz, and S. Charpak, *J. Neurosci. Methods* **111**, 29 (2001).
14. A. G. Yodh and D. A. Boas, *Biomedical Photonics*, T. Vo-Dinh, ed. (CRC Press, Boca Raton, Fla., 2003).
15. D. M. Rector, R. F. Rogers, and J. S. George, *J. Neurosci. Methods* **91**, 135 (1999).
16. J. Jung and M. Schnitzer, *Opt. Lett.* **28**, 902 (2003).
17. H. Yae, S. A. Elias, and T. J. Ebner, *J. Neurosci. Methods* **42**, 195 (1992).
18. K. R. Castleman, *Digital Image Processing* (Prentice-Hall, Englewood Cliffs, N.J., 1979).
19. L. Cauller and B. Connors, *J. Neurosci.* **14**, 751 (1994).